



HAL
open science

Tests of fundamental physics with the Gaia mission through the dynamics of minor planets

Serge Mouret

► **To cite this version:**

Serge Mouret. Tests of fundamental physics with the Gaia mission through the dynamics of minor planets. Physical Review D, 2011, 84, pp.122001. 10.1103/PhysRevD.84.122001 . hal-03785991

HAL Id: hal-03785991

<https://hal.science/hal-03785991>

Submitted on 6 Oct 2022

HAL is a multi-disciplinary open access archive for the deposit and dissemination of scientific research documents, whether they are published or not. The documents may come from teaching and research institutions in France or abroad, or from public or private research centers.

L'archive ouverte pluridisciplinaire **HAL**, est destinée au dépôt et à la diffusion de documents scientifiques de niveau recherche, publiés ou non, émanant des établissements d'enseignement et de recherche français ou étrangers, des laboratoires publics ou privés.

Tests of fundamental physics with the Gaia mission through the dynamics of minor planets

Serge Mouret

*Lohrmann Observatory, Dresden Technical University, Institute for Planetary Geodesy, 01062 Dresden, Germany
and IMCCE, UMR CNRS 8028, Paris observatory, 77 av. Denfert-Rochereau, 75014 Paris, France*

(Received 14 March 2011; published 1 December 2011)

With a launch planned in March 2013, the ESA Gaia mission will scan the whole sky several times during its operational five years. It will provide highly accurate astrometric observations of celestial bodies (at the sub-milli-arcsecond level) not exclusively beyond the Solar System, since about 250 000 asteroids will be observed. Gaia will thus give us the opportunity of performing various valuable tests of fundamental physics by assessing global parameters from the dynamics of minor planets; in this paper, we evaluated its performance from realistic simulated data and a variance analysis carried out from the observation residuals on a data model linearized with respect to the initial position and velocity of each asteroid and the set of global parameters. Currently, the most relevant fits turn out to be for the PPN parameter β ($\sigma_\beta \sim 1.4 \times 10^{-3}$), the temporal variation of the gravitational constant \dot{G}/G ($\sigma_{\dot{G}/G} \sim 3.2 \times 10^{-12} \text{ yr}^{-1}$), the Nordtvedt parameter η ($\sigma_\eta \sim 2.4 \times 10^{-3}$) and the Gm of Jupiter ($\sigma_{Gm_j} \sim 2.9 \times 10^{-15} \text{ au}^3 \text{ d}^{-2}$), which show a low level of correlation. The underestimated astrometric precision used in the simulations and the possibility to combine Gaia data with future accurate ground-based observations foreshadow more accurate determinations.

DOI: 10.1103/PhysRevD.84.122001

PACS numbers: 04.80.Cc, 95.30.Sf, 96.25.De, 96.30.Ys

I. INTRODUCTION

The ESA second-generation astrometric mission Gaia [1], due for a launch in March 2013, will make a new breakthrough in astrometry by performing observations at the sub-milli-arcsecond. In the scope of the solar system, the satellite will observe about 250 000 minor planets down to V magnitude 20 with a precision ranging from a few milli-arcsecond (mas) to about a hundred micro-arcseconds (μas). Furthermore, the positions of about 1×10^9 stars, accurate to a few hundred μas at the limiting magnitude of 20, will be compiled in the Gaia catalogue, and will drastically improve the astrometric reduction of ground-based observations, which depends heavily on the accuracy and completeness of stellar catalogues. Thus, Gaia will boost our knowledge of dynamics of the solar system, and will bring new perspectives in performing clean tests of fundamental physics from asteroid motion analysis.

Using asteroid motions to check properties of general relativity (GR) is not a recent idea: in 1953, Gilvarry [2] suggested to base an observational test of the relativistic perihelion precession on high-eccentric minor planets, and, in particular, (1566) Icarus [3], discovered four years before. This idea was concretized several times [4–7] by estimating a relativity parameter that takes the value one in GR. The best measurements were achieved to a precision of a few percent. The orbital diversity of asteroids has the noticeable advantage of allowing us to disentangle, in many cases, the different origins of certain effects on their motion: in 1965, Dicke [8] had already recognized that asteroids with large inclinations and various semimajor axes enabled us to distinguish between the relativistic

perihelion shift and the possible effects due to the solar oblateness. The huge number of minor planets expected to be very accurately observed by Gaia will offer us the opportunity to extend the applications based on asteroid motion analysis in testing various aspects of general relativity; at present, they cannot compete with the best experiments, such as those from lunar laser ranging (LLR) or planetary ephemerides, on account of the current level of observational accuracy.

In this paper, we focus our attention on the possibility from future Gaia asteroid observations to derive the dynamic solar quadrupole J_2^\odot , the linear time-variation of the gravitational constant \dot{G}/G , the relativistic parameters β and γ in the parametrized post-Newtonian (PPN) formalism, and the Nordtvedt parameter η . A value of η different from zero would import an inequality between the inertial and gravitational mass, and so, a violation of the Strong Equivalence Principle (SEP)—one of the most important consequences of General Relativity (GR) suggested by the solutions of the Einstein field equations. In 1968, Nordtvedt [9] predicted that Trojan asteroids would be particularly sensitive to such a deviation from GR (shift of one arcsecond for $\eta = 1$ towards Jupiter, for the Lagrange points, L_4 and L_5 , that they orbit), and the idea was taken up by Orellana and Vucetich [10,11]. However, both the lack of observations and their low precision precluded them from performing a satisfactory test; the standard deviation was about ± 0.5 . Contrary to what was done before, all the asteroids expected to be observed by Gaia are considered in the estimation process of η .

After describing the observations of minor planets by Gaia in Sec. II and the method used to fit the global parameters in Sec. III, we will provide, for each parameter,

an overview of our current knowledge and the dynamical modeling necessary for their estimation in Sec. IV. In Sec. V, we present the expected precisions for each parameter from a variance analysis based on realistic simulated data—time sequences and geometry of the observations and astrometric precision specific to the satellite. Supplementary information is provided about the most significant asteroids. Finally, a general summary of the results is given in Sec. VI, followed by the perspectives.

II. THE OBSERVATIONS OF MINOR PLANETS WITH GAIA

In March 2013, a Soyuz rocket will lift off from Baikonur with the Gaia satellite on board. One month later, the spacecraft will be inserted into its intended Lissajous orbit around the Lagrange point Earth-Sun L_2 . It will deploy its solar panels and start to operate a continuous scan of the sky for five years. The survey from two telescopes and ruled by a complex scanning law will enable the satellite to perform the astrometric, photometric, and spectroscopic observations of more than 1×10^9 objects, stars forming the majority. A complete description of the mission can be read in Mignard *et al.* [1].

A large number of solar-system objects will be also observed: a systematic exploration of the Gaia transit times for the 542 684 asteroids listed in the ASTORB catalog of Bowell [12] in February 2011 with their orbital elements and absolute magnitudes—necessary to apply the filter to the apparent magnitude—was performed from the first of April 2013, over a period of five years. More than 5.8×10^6 observations were thus found for a total of 241 471 asteroids.

Their distribution according to the number of Gaia observations in Table I shows that about 40% of them will be observed more than 20 times; Gaia will be very likely to

measure the positions of a couple thousand near-Earth asteroids (new detections are expected), which are known to be valuable targets to estimate the dynamic solar oblateness J_2^{\odot} , or the PPN parameters β and γ . Regarding Jovian Trojans, approximately 28% of known objects will be observed; their interest in measuring the Nordtvedt effect η will be, thus, assessed in the framework of such a mission like Gaia (highly accurate measurements over a short time).

In addition to the wealth of asteroid observations, Gaia is going to bring astrometry to the matchless sub-milli-arcsecond level. The positions will be given in longitude λ and latitude β on a reference great circle (RGC) computed from the mean positions of instantaneous scanning circles over one period; as the across-scan (AC) coordinates will be derived with a much lower accuracy than in the along-scan (AL) direction, the latter, solely, will be considered in variance analysis. The AL astrometric precision σ_{λ} is plotted in Fig. 1 as a function of the apparent magnitude of the asteroid. Nevertheless, another parameter has been taken into account: the apparent velocity impacts the centroid error measurement, and so, two cases were defined according to whether or not the AL apparent velocity is smaller than 33,3 mas/s (the largest value found from a very huge sample of main-belt asteroids).

The positional error in Fig. 1 is, however, likely underestimated: the nominal error used to define the Gaia precision is only for one row of CCDs, but nine will form the focal plane of the Gaia telescopes devoted to astrometry. Thus, the asteroid position could be derived from signals collected by several rows, ten in the optimal case if one also considers the row of CCDs for the object detection. Therefore, the formal precision presently estimated might actually be smaller by a factor of 3. More detailed explanations can be read in Mouret and Mignard [13].

TABLE I. Frequency of the future asteroid observations by Gaia. Several groups of minor planets are identified: near-Earth asteroids (NEAs), main-belt asteroids (MBAs), Hilda asteroids, Jovian Trojans, Centaurs, trans-Neptunian objects (TNOs).

observations n	Number of							Total
	NEAs	MBAs	Hildas	Trojans	Centaurs	TNOs	Remainders	
$n < 10$	1093	88 065	495	269	5	1	7263	97 191
$10 \leq n < 20$	307	41 973	225	170	-	-	4007	46 682
$20 \leq n < 30$	124	23 025	124	103	4	1	2184	25 565
$30 \leq n < 40$	103	16 637	63	87	-	-	1309	18 199
$40 \leq n < 50$	33	14 633	80	87	4	2	754	15 593
$50 \leq n < 60$	25	12 929	66	199	2	2	624	13 847
$60 \leq n < 70$	26	9429	50	190	1	4	537	10 237
$70 \leq n < 80$	16	6265	31	133	1	4	387	6837
$80 \leq n < 90$	5	3698	26	58	1	1	202	3991
$90 \leq n < 100$	6	1776	6	44	1	-	105	1938
$n > 100$	7	1260	8	22	-	1	93	1391
Total	1745	219 690	1174	1362	19	16	17 465	241, 471

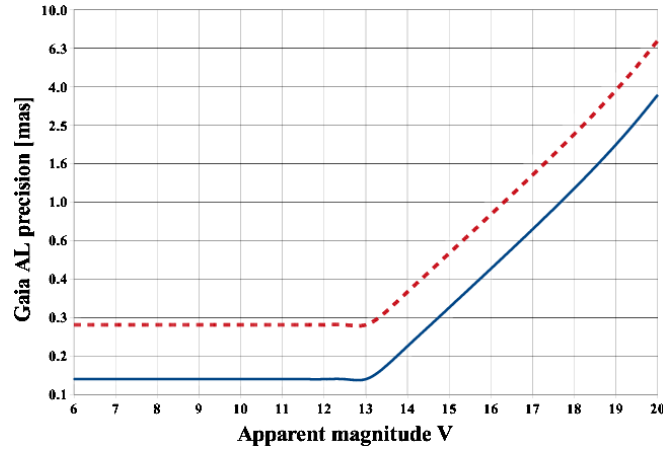


FIG. 1 (color online). The expected along-scan accuracy of individual observations σ_λ as to the asteroid apparent magnitude V and the AL apparent velocity v_{AI} : the continuous line when $v_{AI} > 33,3$ mas/s and the dashed one in the other case.

III. THE METHOD OF ESTIMATING GLOBAL PARAMETERS

Using realistic simulated data, we performed a variance analysis for the position and velocity vectors $\mathbf{u}_0^k = (x_0^k, y_0^k, z_0^k, \dot{x}_0^k, \dot{y}_0^k, \dot{z}_0^k)$ of each asteroid k and a set of global parameters \mathbf{C}_0 itemized in Section IV at the initial epoch $T_0 = \text{JD}2457251.375$ (16th of August 2015) when half the satellite operational time will pass by.

A linear least-square problem is considered to fit the unknown parameters on the observation residuals,

$$\mathbf{W}^{1/2}(\mathbf{O} - \mathbf{C}) = \mathbf{W}^{1/2}\mathbf{A} \begin{pmatrix} \delta\mathbf{u}_0 \\ \delta\mathbf{C}_0 \end{pmatrix} \Rightarrow \begin{pmatrix} \delta\mathbf{u}_0 \\ \delta\mathbf{C}_0 \end{pmatrix} = (\mathbf{A}^T\mathbf{W}\mathbf{A})^{-1}\mathbf{A}^T\mathbf{W}(\mathbf{O} - \mathbf{C}) \quad (1)$$

where $(\mathbf{O} - \mathbf{C})$ are the observed and computed positions in Gaia longitude λ . The corrections to the initial state vector $(\mathbf{u}_0, \mathbf{C}_0)$ are $(\delta\mathbf{u}_0, \delta\mathbf{C}_0)$ with $\mathbf{u}_0 = (\mathbf{u}_0^1, \mathbf{u}_0^2, \dots, \mathbf{u}_0^n)$, n being the total number of asteroids.

The weighting matrix \mathbf{W} is defined by

$$\mathbf{W} = \begin{pmatrix} \ddots & & & 0 \\ & \sigma_{k,i}^{-2} & & \\ & & \ddots & \\ 0 & & & \ddots \end{pmatrix}.$$

Here, $\sigma_{k,i}$ is the error on the position of the k^{th} asteroid at the i^{th} simulated observation date, which is derived from the apparent magnitude and velocity of the asteroid converted to Gaia astrometric precision (see Fig. 1).

The matrix \mathbf{A} contains the partial derivatives of the longitudes λ with respect to the state vector $(\mathbf{u}_0, \mathbf{C}_0)$,

$$\mathbf{A} = \begin{pmatrix} \mathbf{D}_1 & 0 & \cdots & 0 & \mathbf{B}_1 \\ 0 & \mathbf{D}_2 & \ddots & \vdots & \mathbf{B}_2 \\ \vdots & \ddots & \ddots & 0 & \vdots \\ 0 & \cdots & 0 & \mathbf{D}_n & \mathbf{B}_n \end{pmatrix}.$$

Here, \mathbf{D}_k is a $n_{\text{obs}}^k \times 6$ matrix (n_{obs}^k being the number of observations for the asteroid k), which may be defined by

$$[\mathbf{D}_k]_{i,j=1,\dots,6} = \frac{\partial \lambda_i}{\partial \mathbf{u}_0^k} = \begin{pmatrix} \frac{\partial \lambda_i}{\partial x_0^k} & \frac{\partial \lambda_i}{\partial y_0^k} & \frac{\partial \lambda_i}{\partial z_0^k} & \frac{\partial \lambda_i}{\partial \dot{x}_0^k} & \frac{\partial \lambda_i}{\partial \dot{y}_0^k} & \frac{\partial \lambda_i}{\partial \dot{z}_0^k} \end{pmatrix}. \quad (2)$$

It represents the variations of λ_i , the Gaia longitude at the i^{th} observation of the asteroid k , with respect to its position and velocity in rectangular coordinates at the reference time T_0 . As for the $n_{\text{obs}}^k \times p$ matrix \mathbf{B}_k , it consists of the variations of the longitudes λ_i with respect to the p global parameters,

$$[\mathbf{B}_k]_{i,j=1,\dots,p} = \frac{\partial \lambda_i}{\partial \mathbf{C}_0} = \left(\frac{\partial \lambda_i}{\partial C_1}, \dots, \frac{\partial \lambda_i}{\partial C_p} \right). \quad (3)$$

The matrix elements are decomposed with respect to the rectangular coordinates,

$$\frac{\partial \lambda_i}{\partial \mathbf{u}_0^k} = \sum_{q=1}^3 \frac{\partial \lambda_i}{\partial r_q} \frac{\partial r_q}{\partial \mathbf{u}_0^k}, \quad \frac{\partial \lambda_i}{\partial \mathbf{C}_0} = \sum_{q=1}^3 \frac{\partial \lambda_i}{\partial r_q} \frac{\partial r_q}{\partial \mathbf{C}_0},$$

and are then evaluated by analytically computing the quantities $(\partial \lambda_i / \partial r_q)$ while the equations of motion taking into account the perturbations from the planets and Pluto, the solar quadrupole J_2^\odot (see Eq. (8)) and the relativistic effects from the Sun [see Eq. (12)] in the force function \mathbf{F} are numerically integrated,

$$\ddot{\mathbf{r}}(t) = \mathbf{F}(t) \quad (4)$$

together with the variational equations,

$$\frac{d^2}{dt^2} \begin{pmatrix} \partial r_q \\ \partial \mathbf{u}_0^k \end{pmatrix} = \sum_{n=1}^3 \left(\frac{\partial F_q}{\partial r_n} \frac{\partial r_n}{\partial \mathbf{u}_0^k} + \frac{\partial F_q}{\partial \dot{r}_n} \frac{\partial \dot{r}_n}{\partial \mathbf{u}_0^k} \right),$$

$$\frac{d^2}{dt^2} \begin{pmatrix} \partial r_q \\ \partial \mathbf{C}_0 \end{pmatrix} = \frac{\partial F_q}{\partial \mathbf{C}_0} + \sum_{n=1}^3 \left(\frac{\partial F_q}{\partial r_n} \frac{\partial r_n}{\partial \mathbf{C}_0} + \frac{\partial F_q}{\partial \dot{r}_n} \frac{\partial \dot{r}_n}{\partial \mathbf{C}_0} \right).$$

Regarding the temporal variation in the gravitational constant (see Sec. IV C) and a violation of the SEP (see Sec. IV D), the initial values for the associated parameters in the variance analysis process are $\dot{G}/G = \eta = 0$, given that both deviations from the general relativity are not proven.

The formal precisions of the global parameters assessment \mathbf{C}_0 are then given by the diagonal elements of the inverse normal matrix $(\mathbf{A}^T\mathbf{W}\mathbf{A})^{-1}$. In the case of Gaia, the weighted partial derivatives matrix $\mathbf{W}^{1/2}\mathbf{A}$ is huge; more than 200 000 asteroids will be considered. Therefore, handling of the block matrices $(\mathbf{D}_k, \mathbf{B}_k)_{k=1,\dots,n}$ forming the matrix \mathbf{A} is required to compute the covariance elements,

$$\mathbf{c} \text{ cov}(\delta \mathbf{C}_0) = \mathbf{U}^{-1}, \quad (5)$$

$$\mathbf{U} = \sum_{k=1}^n (\mathbf{B}_k' \mathbf{B}_k - \mathbf{B}_k' \mathbf{D}_k (\mathbf{D}_k' \mathbf{D}_k)^{-1} \mathbf{D}_k' \mathbf{B}_k), \quad (6)$$

where n is the total number of treated asteroids. All matrix inversions (see Eqs. (5) and (6)) are obtained through the singular value decomposition, which enables us to diagnose the conditioning of the normal matrix, and so, the stability of the solution.

IV. PARAMETER ESTIMATION AS TESTS OF FUNDAMENTAL PHYSICS

A. The solar quadrupole J_2°

1. Description

Currently, scientists agree that the solar quadrupole moment J_2° is of the order of 10^{-7} according to the most precise estimations from different methods (e.g., helioseismology, figure of the Sun, planetary ephemerides). However, there is still a large scatter in the published values with clearly systematic effects depending on the derivation methods (optical observations, helioseismology, models) and no firm consensus has been reached.

The anomaly of the perihelion motion of Mercury has been known since 1859, thanks to Leverrier [14], but the idea of a distorted Sun for explaining the cause arose only in the 1890s, with Harzer's paper [15] and the independent investigation of Newcomb [16] in 1895. However, this assumption (at least with the magnitude required to account for Mercury anomaly) was ruled out from direct measurements of the oblateness performed during the Venus transits of 1874 and 1882. We may say that the determination of the solar quadrupole J_2° really began in 1966, when Dicke and Goldenberg carried out observations with the Princeton Solar Distortion Telescope. They measured the solar ellipticity for the first time. Their revised estimate, $J_2^\circ = (2.47 \pm 0.23) \times 10^{-5}$ [17], was much larger than the current values. Besides, the astrophysical consequences that it generated were difficult to accept, but rekindled, however, the interest for this subject and originated new investigations of solar interior models.

Two general principles of investigating J_2° can be retained: the astrophysical methods that are based on the physical properties of the studied body, and the dynamical methods, which rest on the analysis of the perturbations that the solar oblateness produces upon the motion of celestial bodies (e.g., asteroids, the Moon and planets). The second approach has the advantage of being directly sensitive to J_2° , regardless of any assumption about the internal structure. However, the historical derivations often provided impossible results: Landgraf calculated in 1992 a negative value, $J_2^\circ = (-6 \pm 58) \times 10^{-7}$ [18], using astrometric observations from 1949 to 1987, and in a very complete review of estimates inferred from the perihelion

shift of Mercury [19], ten negative fits out of 23 can be read. The main causes are certainly the low observational accuracy and systematic errors (that the large observational time-spans increased).

Apart from minor planets, the study of the Moon and planetary motions also gave us the opportunity to constraining the solar quadrupole J_2° . More precisely, the Moon's physical librations due to the solar oblateness were analyzed from the accurate lunar laser-ranging (LLR) data, and Bois and Girard [20] inferred that the value of J_2° was smaller than 3.0×10^{-6} . The planetary ephemerides regularly deliver J_2° estimates. Pitjeva [21] estimated $J_2^\circ = (1.9 \pm 0.3) \times 10^{-7}$ (EPM 2004 planetary ephemerides), Fienga *et al.* [22] found a similar value with $J_2^\circ = (1.82 \pm 0.47) \times 10^{-7}$ (INPOP08), whereas in JPL's ephemerides DE414, $J_2^\circ = (2.34 \pm 0.49) \times 10^{-7}$. The discrepancy could be explained by a difference in the modelling of asteroid perturbations on Mercury and Venus. Nevertheless, Standish gave in a private communication (2000) two estimations that are much closer to those from INPOP08 and EPM 2004: $J_2^\circ = (2.0 \pm 0.4) \times 10^{-7}$ from a particular method detailed in Pireaux and Rozelot [19] $J_2^\circ = (1.9 \pm 0.16) \times 10^{-7}$.

A reliable dynamical estimation of J_2° would be a valuable constraint for the interior model of the Sun and the physical processes that govern its internal structure, its geometry and physics being strongly connected [23,24]. In the field of solar-system dynamics, that would improve orbit determination of the most sensitive celestial bodies (e.g., near-Earth asteroids, Mercury) as well as tests of general relativity; the accuracy in the derivation of the relativistic parameters (PPN) is reduced by their strong correlation with J_2° when they are inferred from the light deflection experiment or dynamical methods.

For all these reasons, deriving precisely J_2° is among the objectives of several future missions. The ESA BepiColombo mission in cooperation with Japan will be launched in about 2014 with the aim of exploring Mercury, the orbit of which is the most sensitive to the solar oblateness among planets. A precision of 10^{-8} is expected [25]. The Astrodynamical Space Test of Relativity using Optical Devices (ASTROD) mission under consideration proposes to test the general relativity using laser interferometric ranging from at least three spacecraft; the formal uncertainty should be of the order of 4.3×10^{-11} [26].

2. Dynamical modelling

The perturbation produced by the solar oblateness, which we denote by $\mathbf{F}^{J_2^\circ}$, is derived from the potential function

$$V_{J_2^\circ} = -\frac{Gm_\odot}{r} \left(\frac{a_e}{r}\right)^2 J_2^\circ P_2(\sin\phi). \quad (7)$$

Here, $P_2(\sin\phi) = (3\sin^2\phi - 1)/2$ is the second Legendre polynomial, ϕ is the latitude of the asteroid in the equatorial frame of the Sun, and $r(=||\mathbf{r}||)$ is its heliocentric distance. The direction of the rotational axis of the Sun is represented by the unit vector \mathbf{K} .

$$\text{As } \sin\phi = \cos\left(\frac{\pi}{2} - \phi\right) = \frac{\mathbf{K} \cdot \mathbf{r}}{r},$$

we have

$$V_{J_2^\circ} = -\frac{1}{2} Gm_\odot a_e^2 \frac{J_2^\circ}{r^5} (3(\mathbf{K} \cdot \mathbf{r})^2 - r^2)$$

and then

$$\begin{aligned} F_i^{J_2^\circ} &= \frac{\partial V_{J_2^\circ}}{\partial r_i} \\ &= -\frac{3}{2} Gm_\odot a_e^2 \frac{J_2^\circ}{r^7} (2(\mathbf{K} \cdot \mathbf{r})r^2 K_i + [r^2 - 5(\mathbf{K} \cdot \mathbf{r})^2]r_i). \end{aligned} \quad (8)$$

The equations of asteroid motion are computed in the ecliptic reference frame. The direction of the solar rotational axis \mathbf{K} is thus expressed in this frame,

$$\begin{aligned} \mathbf{K} &= \mathbf{R}_1(-\epsilon) \times \mathbf{R}_1(-I) \times \mathbf{R}_3(-\theta) \begin{bmatrix} 0 \\ 0 \\ 1 \end{bmatrix} \\ &= \begin{bmatrix} \sin\theta \sin I \\ -\cos\epsilon \cos\theta \sin I + \sin\epsilon \cos I \\ \sin\epsilon \cos\theta \sin I + \cos\epsilon \cos I \end{bmatrix} \end{aligned}$$

where

$$\begin{aligned} \mathbf{R}_1(-I) &= \begin{pmatrix} 1 & 0 & 0 \\ 0 & \cos I & \sin I \\ 0 & -\sin I & \cos I \end{pmatrix}, \\ \mathbf{R}_3(-\theta) &= \begin{pmatrix} \cos\theta & \sin\theta & 0 \\ -\sin\theta & \cos\theta & 0 \\ 0 & 0 & 1 \end{pmatrix}. \end{aligned}$$

Here, $\theta = 90^\circ + \alpha_0$, $I = 90^\circ - \delta_0$ and, α_0 and δ_0 are, respectively, the right ascension and declination of the solar rotational axis in the equatorial reference frame J2000 [27]. The obliquity of the ecliptic $\epsilon = 23^\circ 26' 21''.4119$ [28] is used to pass from the equatorial to the J2000 ecliptic reference frame.

B. The PPN parameters

1. The PPN parameter γ

The parameter γ can be seen heuristically as a measure of the curvature of spacetime by a unit rest mass [29]. The two main tests of the parameter γ are based on the bending of light and the time delay of a signal. Until 1968, every experiment for computing the light deflection was performed during a total solar eclipse. The results were affected by many errors from weather, the change of temperature leading to telescope optical distortions etc. Then, in the early 1970s, the development of radio-interferometry allowed us to achieve a precision of about 0.001 arcsecond: the angular separation of two quasars was monitored while the Sun passed in front of one of the two in order to measure the deflection of its emitted radio waves. Among the very first measurements, we can cite Seielstad *et al.* [30] and Muhleman *et al.* [31], who, in 1970, provided, respectively, $(1 + \gamma)/2 = 1.01 \pm 0.12$ and $(1 + \gamma)/2 = 1.04_{-0.10}^{+0.15}$. Then, the very-long-baseline radio interferometry (VLBI) became the most accurate tool and achieved accuracies better than 100 μas in deriving angular separations and their variations. From almost 2×10^6 VLBI observations (from 541 radio sources spread out among 87 VLBI sites), Shapiro *et al.* (2004) measured $\gamma - 1 = (-1.7 \pm 4.5) \times 10^{-4}$ [32]. The derivation precision was then improved: γ was found to be unity within 1.2×10^{-4} [33]. However, this method is not a ‘‘pure’’ bending-of-light experiment in so far as the Shapiro effect [34] is routinely accounted for in VLBI observations contrary to the measurement performed by Fomalont *et al.* (2009), which provided $\gamma - 1 = (2 \pm 3) \times 10^{-4}$ [35].

The other general test of γ consists in measuring the time delay of a signal (deviation from the Newtonian framework) known as the Shapiro effect, in the round-trip travel time of a radar signal due to the presence of a massive body near its route. We can count two types of experiment according to the reflector: the latter takes the form either of a planetary surface (e.g., Venus or Mercury) or of a piece of electronic equipment on board a spacecraft in charge of retransmitting the signal to the Earth. The Cassini experiment based on Doppler tracking of the spacecraft, which was heading for Saturn, provided one of the most precise measurements with $\gamma - 1 = (2.1 \pm 2.3) \times 10^{-5}$ [36]. Nevertheless, the data processing algorithm did not take into account the orbital motion of the Sun, what sparked off several discussions [37,38].

The parameter γ was also fitted by analyzing the relativistic effects from the Sun on planetary motion. It was estimated along with the parameter β accurately to 2×10^{-4} [39]. However, the correlation between both parameters was most likely high since Pitjeva [40] found a correlation of 84% for a similar fit.

Several future missions will improve the γ measurement accuracy: BepiColombo expects a precision of $\sim 2 \times 10^{-6}$ [41] by determining the perihelion shift of Mercury’s orbit

and measuring the time delay and Doppler shift. However, the most promising missions are LATOR [42]—the deflection of light will be measured by laser interferometry between two micro-spacecraft whose lines of sight pass close by the Sun—and ASTROD [26], which predicts an accuracy of 10^{-9} . Earlier than the end of these missions, Gaia should provide a very competitive estimate accurate to about 10^{-6} [43] from a bending-of-light experiment. The same process was used from the Hipparcos astrometric data to achieve the best determination of γ in the visible: $\gamma = 0.997 \pm 0.003$ [44].

2. The PPN parameter β

In the PPN formalism, the parameter β is described as a measure of the nonlinearity in the superposition law for gravity [29]. The primary source for its assessment follows from the drift in the perihelion of solar-system objects. It is produced by the relativistic effects from the Sun at the rate of

$$\dot{\omega} = (2 + 2\gamma - \beta) \frac{n}{a(1 - e^2)} \frac{Gm_{\odot}}{c^2}, \quad (9)$$

where ω is the argument of perihelion, a the semimajor axis of the perturbed body, e its eccentricity, n its mean motion, and c the speed of light. Thus, analyzing the motion of bodies orbiting the Sun offers a dynamic constraint of β . Furthermore, its strong correlation with γ can be overcome, the latter having been accurately estimated from other methods mentioned in Sec. IV B 1. Currently, the most precise estimations of β , uncertain to $\sim 1 \times 10^{-4}$, were obtained from the planetary observations: the fits were performed along with the solar quadrupole J_2^{\odot} in Fienga *et al.* [45] and γ in Pitjeva [21].

In the PPN formalism, β can be also measured from the test of the strong equivalence principle. This parameter is linked to the Nordtvedt parameter η and the PPN parameters ($\beta, \gamma, \xi, \alpha_1, \alpha_2, \zeta_1, \zeta_2$) by the relationship [46]

$$\eta = 4\beta - \gamma - 3 - \frac{10}{3}\xi - \alpha_1 + \frac{2}{3}\alpha_2 - \frac{2}{3}\zeta_1 - \frac{1}{3}\zeta_2, \quad (10)$$

which, in fully conservative, Lorentz-invariant theories of gravity, can be reduced to

$$\eta = 4\beta - \gamma - 3. \quad (11)$$

From the previous equation, the LLR data enabled us to estimate $\beta - 1$ to $(1.2 \pm 1.1) \times 10^{-4}$ [47]. Including the SEP in the β fit can be of particular interest in reducing the strong correlation between β and the solar quadrupole J_2^{\odot} if the fit is also based on the analysis of the relativistic perihelion shift. This was investigated for the BepiColombo radio science experiment [41], and a precision of 2×10^{-6} is expected for the estimation of β while the Nordtvedt parameter η would be constrained within $\sim 10^{-5}$.

3. Dynamical modelling

In the heliocentric equations of motion, the relativistic terms produced by a nonrotating spherically-symmetric Sun are given by the Schwarzschild solution, which in the PPN formalism and isotropic coordinates take the form [48],

$$F_i^{\mathcal{R}} = \frac{Gm_{\odot}}{c^2} \left[\left(2(\beta + \gamma) \frac{Gm_{\odot}}{r^4} - \gamma \frac{(\dot{\mathbf{r}} \cdot \dot{\mathbf{r}})}{r^3} \right) r_i + 2(\gamma + 1)(\mathbf{r} \cdot \dot{\mathbf{r}}) \frac{\dot{r}_i}{r^3} \right], \quad (12)$$

where \mathbf{r} and $\dot{\mathbf{r}}$ are, respectively, the position and velocity vectors of the asteroid.

C. The time-variation of the gravitational constant

Dirac was among the first to point out a possible variation of the constant of gravitation G . This hypothesis originates in the fact that the combination of the gravitational constant G , the reduced Planck constant \hbar and the Hubble constant H_0 as

$$\left(\frac{\hbar^2 H_0}{Gc} \right)^{1/3} \simeq m_{\pi}, \quad (13)$$

is close to the mass of the pi-meson (elementary particle) m_{π} [49]. Regarding this numerical coincidence as significant is problematic for many cosmological models, which consider H_0 as nonconstant but a function of the age of the universe t_u . Instead of reformulating the atomic and nuclear physics, Dirac thus stated that G decreases with time at the rate of

$$\dot{G}/G = -3H_0 = -t_u^{-1}.$$

Theories of gravitation inspired by the idea of a time-varying G were attempted. The most accomplished was proposed by Brans and Dicke [50] in 1961, when they replaced $1/G$ by a scalar field which can vary in space and time.

Several methods can provide a constraint on \dot{G}/G . If we consider measurement precision and model validity, the analysis of LLR data yields the best estimations: \dot{G}/G was measured at the level of $(4 \pm 9) \times 10^{-13} \text{ yr}^{-1}$, showing for the highest correlation a value of 0.74 with the diurnal tidal dissipation parameter [47]; the accuracy was then improved to reach a standard deviation of $3 \times 10^{-13} \text{ yr}^{-1}$ [51]. More precise estimations better than $\sim 0.1\%$ of the inverse of the universe age ($\sim 7.3 \times 10^{-14} \text{ yr}^{-1}$) are expected with the new APOLLO ranging station [52]. However, the increase of the derivation accuracy requires to refine the dynamical modelling: Williams *et al.* [52] pointed out the fact that testing \dot{G}/G can be influenced by the solar mass loss ($\sim -7 \times 10^{-14} m_{\odot} \text{ yr}^{-1}$) given the impossibility to discriminate between a variation in G and m_{\odot} , and the thermal reradiation from the Earth and

Moon has to be considered for accuracies below 10^{-14} yr^{-1} .

The study of the Big-Bang nucleosynthesis, helioseismology, pulsar timing data and planetary radar-ranging measurements [53] also allow to measure \dot{G}/G . Using the observations of Mars (Viking landers, Mariner 9), Venus and Mercury (radar) and LLR data, Hellings *et al.* [54] measured $\dot{G}/G = (2 \pm 4) \times 10^{-12} \text{ yr}^{-1}$. The authors indicated that the lack of knowledge in asteroid masses was the major uncertainty in the estimation of \dot{G}/G . Therefore, the fits from planetary observations will gain in accuracy when Gaia has derived the masses of more than 150 massive asteroids [55], resulting mainly in improving the Martian ephemeris [56]. A more recent estimate by Pitjeva [39] who used a huge set of planetary observations, reached a precision of $5 \times 10^{-14} \text{ yr}^{-1}$.

In the literature, formulas can be read about the secular variations of osculating elements (semimajor axis a , mean motion n and mean longitude λ) due to the gravitational “constant” decreasing in time. They are based on a property demonstrated by Mestschersky [57,58], which states that the classical two-body problem can be reducible to quadratures if the constant of gravitation is expressed as

$$G = (b_1 + b_2 t)^{-1},$$

where b_1 and b_2 are constants. Then, Vinti [59] calculated the following expressions by assuming $G(t) \sim (k + t)^{-1}$,

$$\frac{1}{2} \frac{\dot{n}}{n} = -\frac{\dot{a}}{a} = \frac{1}{2n} \frac{\dot{\lambda}}{\lambda} = \frac{\dot{G}}{G}.$$

In the framework of Gaia, we consider a linear variation in time of G ,

$$G_{\text{eff}}(t) = G + \dot{G}(t - t_0), \quad (14)$$

where t_0 is a reference time. In terms of secular effect, we can notice a change in the mean anomaly M at the time t by an amount of (see Appendix A),

$$\Delta M = n \frac{\dot{G}}{G} m_{\odot} (t - t_0)^2, \quad (15)$$

where n is the asteroid mean motion at the time t_0 .

D. Testing the Strong Equivalence Principle

1. Description

The equivalence principle (EP) contributed to the foundation of the Theory of General Relativity. It states that the inertial mass m_I , which measures the resistance of a body to a change of its motion, is equal to the gravitational mass m_G that scales its acceleration in an external gravitational field. One hypothesis of the EP says that the acceleration of any freely falling test body is not determined by its composition or structure. Thus, we can separate this principle into two forms according to the internal interactions contributing identically to the inertial and gravitational

masses. The weak form is based on the strong, weak and electromagnetic forces, while the strong one also includes the gravitational interaction.

The very first tests by Newton, and then Bessel, compared the periods of pendulum differing in masses and compositions without showing a discrepancy. Then Baron Loránd von Eötvös devised a more sophisticated experiment based on a torsion-balance [60] that the Princeton group of Dicke redesigned. The gravitational accelerations of gold and aluminum turned out to be equal to one part in 10^{11} [61]. Currently, the weak equivalence principle was tested to a precision of 10^{-13} by measuring the fractional differential acceleration between beryllium and titanium [62,63]. Nevertheless, the objects tested in the laboratory are by far too small for a test of the Strong Equivalence Principle (SEP) contrary to astronomical bodies which show a significant contribution of the gravitational self-energy to their masses (see Table II).

The violation of the SEP was first envisaged by Dicke [67], but it is Nordtvedt who independently discovered and investigated carefully the hypothesis [9,68,69]. In the PPN formalism, the Nordtvedt effect is generalized by

$$\frac{m_G}{m_I} = 1 + \Delta = 1 + \eta \frac{E_g}{m_r c^2} \quad (16)$$

where η is a dimensionless constant known as the Nordtvedt parameter. m_r is the rest mass (inertial mass when the body is at rest),

$$m_r = \int_V \rho(\mathbf{x}) d^3 \mathbf{x}.$$

Here, $\rho(\mathbf{x})$ is the mass density of the body, \mathbf{x} the vector from the center of mass to a point in the volume. Δ is the correction term associated to the body depending on its gravitational self-energy,

$$E_g = -\frac{1}{2} G \int \frac{\rho(\mathbf{x}) \rho(\mathbf{x}')}{|\mathbf{x} - \mathbf{x}'|} d^3 \mathbf{x} d^3 \mathbf{x}' = -\frac{1}{2} \int V(\mathbf{x}) \rho(\mathbf{x}) d^3 \mathbf{x}, \quad (17)$$

TABLE II. Correction terms for massive astronomical bodies ($\eta = 1$) and laboratory objects as a comparison.

Body	Δ	Body	Δ
Mercury	-6×10^{-11}	Jupiter	-1.2×10^{-8}
Venus	-3.6×10^{-10}	Saturn	-4.3×10^{-9}
Earth ^a	-4.2×10^{-10}	Uranus	-1.5×10^{-9}
Moon	-1.9×10^{-11}	Neptune	-1.9×10^{-9}
Mars	-8.4×10^{-11}	Ceres ^b	-9×10^{-13}
Laboratory objects $\sim 10^{-25}$			

^aThe numerical evaluation by Anderson *et al.* [64] from the Earth model of Allen [65] gives a close result: $\Delta = -4.6 \times 10^{-10}$.

^bA mean radius of 467.9 km is used [66].

where $V(\mathbf{x})$ is the gravitational potential. In the solar system, the correction term Δ for the Sun is by far the largest if the SEP is violated. A numerical evaluation based on the standard solar model [70] yields

$$\Delta_{\odot} \sim -3.52 \times 10^{-6} \eta.$$

Regarding the other massive celestial bodies (see Table II), the internal gravitational potential of an homogeneous sphere of radius R with a density ρ can be used,

$$V(r) = 2\pi G\rho \left(R^2 - \frac{1}{3} r^2 \right), \quad (18)$$

to approximate their gravitational self-energy, and then the associated correction term

$$\Delta = -\frac{3}{5} \frac{Gm_r}{c^2 R} \eta. \quad (19)$$

If the gravitational self-energy disobeys the equivalence principle, Earth is falling toward the Sun with an acceleration different from that of the Moon. An orbit polarization of the Earth satellite can thus be noticed directed along the Earth-Sun line [71] with an oscillation of the distance Earth-Moon [72],

$$\delta r(t) = 13\eta \cos(\omega_0 - \omega_s)t [\text{meters}].$$

Here, ω_0 and ω_s are, respectively, the angular velocities of the assumed circular unperturbed orbits of the Moon and the Sun around the Earth. The cosine argument represents the angle between the Earth-Moon and Earth-Sun vectors at the time t . Since the first LLR measurements in 1969, their analysis has provided the most accurate test of the SEP: the precision currently reached is $|\eta| = (4.4 \pm 4.5) \times 10^{-4}$ [47], and should be pushed to a few parts in 10^5 [52] with the Apache Point Lunar Laser-ranging Operation (APOLLO) project [73] by achieving the millimetric range precision.

In his first paper, Nordtvedt [9] suggested the observation of Trojan asteroids as a possible experiment: the Nordtvedt effect would produce a movement of the Lagrange points L4-L5 toward Jupiter by an amount of

$$\delta r = \frac{1}{3} \Delta_{\odot} R_{\odot J} \sim 912.7 \text{ km} (\eta = 1)$$

where $R_{\odot J}$ is the Sun-Jupiter distance. Orellana and Vucetich [11] implemented the idea from observations of the first 12 Trojan asteroids over large periods of time ranging from 64 to 84 years. The Nordtvedt parameter was then measured to $\eta = -0.56 \pm 0.48$ with an analysis of external errors. The lack of accuracy in the astrometric observations was the major barrier to achieving a competitive derivation of η . Other tests drew inspiration from three-body configurations such as using radar observations of 2:1 resonant asteroids with Jupiter [74].

2. Dynamical model

The basic post-Newtonian equations of motion for a system of mass-monopoles can be described by the well-known Einstein-Infeld-Hoffmann (EIH) equations. Their expression in the PPN formalism can be read in Will [46]. If the SEP is violated, only the Newtonian part of the equations of motion is modified by Eq. (16) in the case of spherically-symmetric, stationary bodies and relativistic terms expressed to the order c^{-2} . In barycentric coordinates, they may be written for a body k as,

$$\frac{d^2 \mathbf{x}_k}{dt^2} = -(1 + \Delta_k) \sum_{B \neq k} Gm_B \frac{\mathbf{x}_{kB}}{|\mathbf{x}_{kB}|^3} \quad (20)$$

where \mathbf{x}_k and Δ_k , are, respectively, the position vector and the correction term from Eq. (16) of the body k , $\mathbf{x}_{kB} = \mathbf{x}_k(t) - \mathbf{x}_B(t)$, and m_B is the mass of the body B .

Changing the equations of motion into heliocentric coordinates allows us to introduce the solar correction term Δ_{\odot} from the Nordtvedt effect. Subtracting the barycentric acceleration of the Sun (see Eq. (20)) from those of an asteroid a gives the heliocentric equations of dynamics,

$$\begin{aligned} \frac{d^2 \mathbf{r}_a}{dt^2} = & -G((1 + \Delta_a)m_{\odot} + (1 + \Delta_{\odot})m_a) \frac{\mathbf{r}_a}{|\mathbf{r}_a|^3} \\ & - \sum_{B \neq a, \odot} Gm_B \left((1 + \Delta_a) \frac{\mathbf{r}_{aB}}{|\mathbf{r}_{aB}|^3} + (1 + \Delta_{\odot}) \frac{\mathbf{r}_B}{|\mathbf{r}_B|^3} \right) \end{aligned} \quad (21)$$

where \mathbf{r}_a and \mathbf{r}_B are, respectively, the heliocentric position vectors of the asteroid and the perturbing body B which here are the planets, $\mathbf{r}_{aB} = \mathbf{r}_a(t) - \mathbf{r}_B(t)$.

In Eq. (21), the Nordtvedt effect appears in several terms but with large differences in magnitude. It is thus relevant to carry out a selection of the most significant terms in estimating η according to the magnitude, given the short observational timespan of the Gaia mission. We roughly first estimated the correction factor Δ for 542 684 asteroids from the Astorb database. Each asteroid is considered as a spherical body with a mass m and a homogeneous density ρ . The mass used is either a direct measurement or an estimation from a density assumed to 2.5 g cm^{-3} and a volume concluded from the diameter as a function of the absolute magnitude H and the geometric visible albedo [75]. Under the assumption of a spherical asteroid, the correction term Δ is $\propto m^{2/3} \rho^{1/3}$. Mass is the deciding parameter for a strong correction factor. Compare now the magnitudes of the terms containing the Nordtvedt parameter:

$$\begin{aligned} \varphi_1 &= Gm_{\odot} \Delta_a / |\mathbf{r}_a|^2, & \varphi_2 &= Gm_a \Delta_{\odot} / |\mathbf{r}_a|^2, \\ \psi_1^B &= Gm_B \Delta_a / |\mathbf{r}_{aB}|^2, & \psi_2^B &= Gm_B \Delta_{\odot} / |\mathbf{r}_B|^2. \end{aligned} \quad (22)$$

The maximum values for φ_1 and φ_2 from the above equations were found for asteroid (1) Ceres, which combines a

large mass with a close heliocentric distance in comparison with the massive dwarf planets beyond Neptune. Compared with the mean value of ψ_2^J , which appears in the Jovian perturbations and is by far the largest among the perturbations of its kind, the quantities φ_1 and φ_2 are much smaller:

$$\psi_2^J/\varphi_1 > 10^3 \quad \text{and} \quad \psi_2^J/\varphi_2 > 2 \times 10^6.$$

Regarding the quantity ψ_1^B , it varies with the distance of the asteroid to the planet B . We must consider different groups of minor planets according to the encounters that they can experience with planets. The first one is the population of near-Earth asteroids, and only the most massive inner planet is used for computations. Among 7614 NEAs, the asteroid showing the largest correction factor has to fly past Earth at a distance shorter than 5.3×10^{-6} au ($\sim 0.05\%$ of the terrestrial Hill sphere radius) so that at the encounter time, ψ_1^{\oplus} is equal to the mean value of ψ_2^J . As to the asteroids having an orbit close to Jupiter's (e.g., Hilda asteroids, Trojans), the planetary distance has to be smaller than 6.5×10^{-4} au ($\sim 0.19\%$ of the Jovian Hill sphere radius). Thus, the planetocentric distances necessary for the term ψ_1^B to be also retained in constraining η are too small: the probability to observe such small distances between an asteroid and the above-mentioned planets during the Gaia mission is extremely low, and even if that was so, it would be risky to use the observations of the offending asteroid to test the SEP; in such cases of close approaches, the very strong gravitational perturbations caused by the planet prevent us from accurately fitting parameters because their modelling becomes too sensitive to the initial conditions. As a conclusion, the terms depending on the heliocentric position of planets, and, in particular, Jupiter, are easily the most significant in the estimation of the Nordtvedt parameter. In the framework of Gaia, the dynamical model in analyzing the Nordtvedt effect may be thus expressed as

$$\frac{d^2 \mathbf{r}_a}{dt^2} = -G(m_{\odot} + m_a) \frac{\mathbf{r}_a}{|\mathbf{r}_a|^3} - \sum_{B \neq a, \odot} \left(Gm_B \frac{\mathbf{r}_{aB}}{|\mathbf{r}_{aB}|^3} + (1 + \Delta_{\odot}) Gm_B \frac{\mathbf{r}_B}{|\mathbf{r}_B|^3} \right). \quad (23)$$

We can notice that the masses of planets are factors inseparable from the force due to the Nordtvedt effect (see Eq. (23)). They will thus be considered in the variance analysis in order to evaluate their correlations with η . When comparing the values of planetary masses and their mean distance to the Sun, modelling the anomalous ‘‘Nordtvedt’’ perturbation only through the perturbations by Jupiter is fully sufficient. That was confirmed by numerical simulations in Sec. V.

3. Discussion

When drawing a distinction between the inertial and gravitational masses, we must pay attention to the nature

of the estimated masses of the bodies that perturb the asteroid motion. Regarding planets, their masses are computed by analyzing their gravitational perturbations on their natural satellites or space probes passing nearby, and in consequence, they are gravitational masses. Regarding the Sun, its Gm is estimated by analyzing its effect on the motions of the planets (gravitational mass) as well as from the light-times through the Shapiro effect (gravitational mass). However, this case is slightly different from planets: for historical reasons, Gm_{\odot} is first held to a fixed value in units of $\text{au}^3 \text{day}^{-2}$ and the position and velocity of the planets are integrated in units of au and au day^{-1} , in order to be then fitted to observations (mainly round-trip light-time in seconds) along with the scale factor converting au to km. Then, Gm_{\odot} can be evaluated in $\text{km}^3 \text{s}^{-2}$. Even if the derivation is not really direct, numerical tests showed that the result obtained is similar to a fit of the solar Gm with an au fixed (Folkner, personal communication). In INPOP08 [22], that was also checked. In a near future, the fit of Gm_{\odot} with an au fixed should replace the current procedure that is described above.

As seen in Sec. IV D 1, the violation of the SEP in the case of spherically-symmetric bodies results only in a difference between the inertial and gravitational masses defined by Eq. (16) and so, in Eq. (20). Nevertheless, the nonstationarity of bodies (e.g., radial oscillation) can produce a violation of the SEP in the case where $\gamma \neq 1$, and also $\beta \neq 1$ if several nonstationary bodies are considered: the resulting impact in the translational equations of motion investigated by Vlasov [76] is given in Eq. (9.4.7) of their paper. New terms also appear in the formulation of the gravitational mass. It will be interesting to consider the radial oscillations of the Sun to test the SEP: we should determine if these effects can be important in the violation of the SEP according to the recent estimations of γ and then if they are so, redesign the test of the SEP by taking account the new terms in the equations of motion from these new effects.

V. RESULTS

A. Expected formal uncertainties

Using realistic simulated data (see Sec. II), we estimated, for each parameter previously presented, the formal precisions that we can expect by performing a global fit from Gaia data. In addition, a careful analysis of the covariance matrix allowed us to detect the asteroids not suitable for the global least squares inversion, the low number and bad distribution of observations being the main reasons. Once these 129 122 minor planets had been discarded, 112 349 minor planets remained for the variance analysis. The Gm of Jupiter was added to the unknown parameters by reason of its potential strong correlation with the Nordtvedt parameter η . The general result is presented in Table III, supplemented by the best current estimations of each parameter as a comparison and those

TABLE III. Overview of the Gaia performance in constraining the following global parameters: the PPN parameters β and γ , the solar quadrupole J_2^\odot , the time-variation of the gravitational constant \dot{G}/G , the Nordtvedt parameter η and the Gm of Jupiter.

Parameter	Initial value	the best current estimates		Formal precisions		
				from Gaia (simulations)	future missions	
β	1 ^a	$\sim 10^{-4}$	Planetary ephem.	1.44×10^{-3}	2×10^{-6}	BepiColombo [41]
γ	1 ^a	2.3×10^{-5}	Cassini [36]	7.90×10^{-4}	10^{-9}	ASTROD [26]
J_2^\odot	2×10^{-7}	$\sim 5 \times 10^{-8}$	Planetary ephem.	1.71×10^{-7}	10^{-8}	BepiColombo [25]
\dot{G}/G [yr ⁻¹]	0 ^a	9×10^{-13}	LLR [47]	3.18×10^{-12}	$\sim 7.3 \times 10^{-14}$	LLR [52]
η	0 ^a	4.5×10^{-4}	LLR [47]	2.36×10^{-3b}	$\sim 10^{-5}$	LLR [52]
Gm_j [au ³ d ⁻²]	2.82×10^{-7}	3.35×10^{-15}	Jovian satellites ^c	2.89×10^{-15}		

^aTheoretical value in general relativity,

^b $\Delta_\odot = -3.52 \times 10^{-6} \eta$

^cJacobson, R. A. 2005. "Jovian Satellite ephemeris–JUP230" private communication.

that other missions will achieve. The correlation coefficients are given in Table IV. Those for β and γ are noticeably similar in magnitude, and hence the parameter γ do not appear in the correlation matrix. We separated the parameters β and γ in the variance analysis because they are very strongly correlated, and it is more relevant to fit only one while the other is held to a value derived from another method. The variance analysis results lead us inclined to assessing β given that γ can be derived differently and more precisely: the bending-of-light experiment by Gaia should allow us to achieve a precision of about 10^{-6} [43] instead of 8×10^{-4} from the Gaia asteroid observations (see Table III). Regarding the Nordtvedt effect, numerical simulations showed us that only the effects from a violation of the SEP in the Jovian perturbations on asteroid motion was important in appraising η : 1 order of magnitude is lost in the formal precision, when Jupiter is removed from the set of eight planets. More precisely, the precision on η could decrease to only $\sigma_\eta^l = 2.8 \times 10^{-2}$ (fitted along with β , J_2^\odot and \dot{G}/G).

Gaia will make a breakthrough in tests of fundamental physics from the dynamics of asteroids: even if the expected precisions are not better than the best current ones (see Table III), the analysis of Gaia data will first provide rather competitive and valuable constraints on most of them. The results could even be improved by a factor ~ 3 at most, knowing that the astrometric precision used in the simulations was underestimated (see Sec. II). Furthermore, the systematic errors will be limited by the short observational time-span (five years) and a very complete dynamical model; the perturbations from many massive asteroids, the relativistic effects from the Sun, and also the planets in certain cases, as well as nongravitational forces will be modeled. Thus, the fit accuracy will be ensured. Using a large set of asteroid orbits will allow us to decrease the correlations between the fitted parameters: the coefficients listed in Table IV are low except for the correlations between J_2^\odot and β as expected (~ 0.57), and to a much lesser degree between the Nordtvedt parameter η

and both \dot{G}/G and Gm_j with respective values of -0.18 and 0.2 . Nevertheless, the current estimated uncertainty for J_2^\odot does not show its assessment with Gaia as relevant (the standard deviation being close to current estimates). Holding this parameter to a nominal value from future missions like BepiColombo turns out to be the wisest solution for the moment. Another point to stress is that Gaia should provide a competitive estimate of the Gm of Jupiter with the best current one obtained from natural satellite motion analysis. The formal precision should even be better given the underrated Gaia astrometric performance (see Sec. II).

A point to keep in mind is that these parameters can be measured by other methods, with a high accuracy at times: the dynamical model that will be used for Gaia can thus be put to the test. As an example, a precision of 10^{-5} is predicted for η from the LLR experiments with the APACHE telescope [52], and a deviation between the latter and the Gaia measurement could shed light on inadequacies in the dynamical model.

Two mission scenarios have been likewise examined: the first one plans a launch delay of one year with the same mission duration (five years) and the second one an operational-time extension by one year. The new expected standard deviations for our set of global parameters are given in Table V. We can notice that the mission postponement does not have a significant impact on the fit precisions, as valuable asteroids are always observed by the satellite. Nevertheless, an additional year for the mission

TABLE IV. Correlation matrix for the fit of the parameters listed in Table III.

	β	J_2	η	Gm_j	\dot{G}/G
β					
J_2^\odot	0.568				
η	-0.064	-0.035			
Gm_j	0.003	-0.010	0.203		
\dot{G}/G	0.031	0.023	-0.183	-0.047	

TABLE V. Uncertainty estimates as to different Gaia mission scenarios.

Parameter	Current Planning: 20132018	Scenarios	
		Launch delayed for one year: 20142019	Mission extended by one year: 20132019
σ_β	1.44×10^{-3}	1.28×10^{-3}	7.42×10^{-4}
σ_γ	7.90×10^{-4}	6.71×10^{-4}	3.79×10^{-4}
$\sigma_{J_2^\circ}$	1.71×10^{-7}	1.64×10^{-7}	4.64×10^{-8}
$\sigma_{\dot{G}/G}$ [yr ⁻¹]	3.18×10^{-12}	2.43×10^{-12}	1.08×10^{-12}
σ_η	2.36×10^{-3}	2.15×10^{-3}	9.90×10^{-4}
σ_{Gm_j} [au ³ d ⁻²]	2.89×10^{-15}	3.02×10^{-15}	1.38×10^{-15}

would allow us to improve the precisions by factors within 1.9–3.7.

B. The most valuable asteroids

In this part, we focus on the most significant asteroids in estimating each parameter: the expected precisions are computed for the set of parameters listed in Table III but by removing solely one asteroid each time. Thus, the increase in the estimate uncertainty of each parameter because of the removal allow us to assess the importance of each asteroid in the process of fitting and to rank them relative to their contribution. This can be useful to better appraise the solution accuracy and to refine the dynamical model if need be (e.g., modelling nongravitational forces for certain NEAs).

In Fig. 2, the increase in the standard deviation for each parameter was drawn as a function of the number of the asteroids removed from the fit and previously ranked by decreasing contribution to each estimation. A few significant Earth-crossing asteroids provide most of the

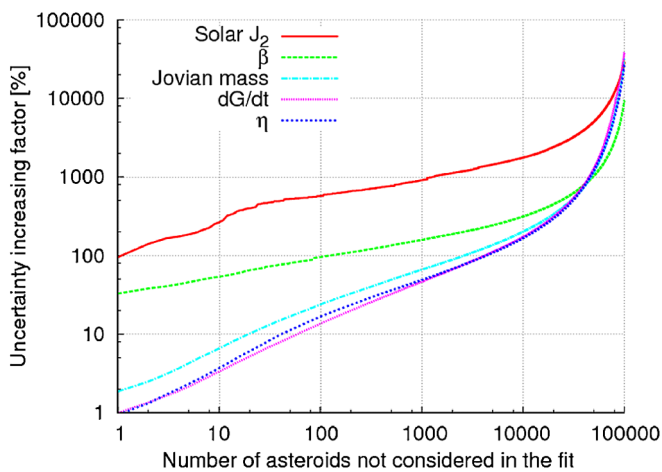


FIG. 2 (color online). Variation of the uncertainty in the derivation of (J_2° , β , \dot{G}/G , η , Gm_j) relative to the asteroids removed from the fit. They were first ranked by decreasing contribution to the estimation of each parameter.

information on the values of β and J_2° . They are listed in Table VI where, withal, we can read the semimajor axes and eccentricities of the asteroids, their theoretical perihelion precession rates (from relativity and the solar oblateness), some observation aspects of them by Gaia and their contribution to estimating β and J_2° . In addition, we provide some information about the Yarkovsky effect given that it may be an important component in NEA orbit determination: we evaluated the capability of Gaia to detect a secular drift in the semimajor axis \dot{a} from this nongravitational force using the same procedure detailed in Ref. [13]; we thus yield the uncertainty on \dot{a} from the present simulated Gaia data (see Sec. II), and its ratio to an estimated \dot{a} . The latter was numerically computed from formulas used in the modelling of the Yarkovsky perturbations by Vokrouhlický [77,78] except for two asteroids, (2100) Ra-Shalom and (85953) 1999 FK21, the Yarkovsky effect in their motions having already been revealed [79]. Table VI shows three NEAs as being by far the most important in β and J_2° derivations: (137924) 2000 BD19, (66391) 1999 KW4 and (3200) Phaethon. Even if these minor planets do not have the optimal characteristics to be strongly sensitive to the Yarkovsky forces (e.g., their diameters, from the MPC or inferred from their absolute magnitudes and geometric visible albedos [75], are larger than 1 km), our scanty knowledge of other important physical parameters does not allow us to accurately assess the Yarkovsky acceleration, and to label it as negligible for the β and J_2° fits. Therefore, the Yarkovsky signature in their orbits will be investigated from the Gaia observations through the secular variation in the semimajor axis, which might be estimated to a precision of $\sim 10^{-4}$ au Myr, for the three NEAs above-mentioned. However, complementary ground-based observations (e.g., radar, photometric) would be valuable to increase the ability to detect and model the Yarkovsky forces, and consequently to get more accurate fits.

The information about the other parameters (\dot{G}/G , η and Gm_j) is chiefly yielded by several thousands of asteroids, most of them lying in the main-belt (see Fig. 3). Regarding the Nordtvedt effect, MBAs are easily the main source of knowledge about η : we can achieve a precision of

TABLE VI. The most contributive 20 asteroids to the estimations of β and J_2° . Their orbital semimajor axis a and eccentricity e are provided with the perihelion precession rate $\dot{\omega}$ (from relativity and the solar oblateness), the total number of Gaia observations and, in parentheses, the quantity of cases with a “critical” apparent along-scan velocity (see Sec. II), the observation arc and the mean apparent magnitude $meanV$. In the next two columns, we give the increasing factor in the uncertainty of their estimates if the asteroid i is not included in the process of fit, and its cumulative value. The last two columns are devoted to the Yarkovksy effect: first, we can read the sensitivity of Gaia to reveal this effect through the secular drift in the semimajor axis \dot{a} , and then we relate the formal uncertainty to a rough numerical estimation of \dot{a} .

n° IAU	Asteroid i name	a [au]	e	Perihelion shift $\dot{\omega}_\beta$ ["/100yr]	Gaia observations			Uncertainty increasing		Yarkovsky effect		
					number	arc [yr]	Mean V	factor in the fit of β [%]	factor in the fit of β [%]	σ_a^{Gaia} [$\times 10^{-4}$ auMyr]	$\ \dot{a}\ /\sigma_a^{Gaia}$ [$\times 10^{-4}$ auMyr]	
66391	1999 KW4	0.64	0.69	22.05	37	(10)	4.2	17.7	12.31	12.31	1.01	1.85
137924	2000 BD19	0.88	0.90	26.80	34	(5)	4.4	19.0	12.13	32.81	6.25	0.35
3200	Phaethon	1.27	0.89	10.11	74	(15)	4.1	18.2	1.94	38.01	1.73	0.39
105140	2000 NL10	0.91	0.82	14.43	72	(4)	4.2	18.8	1.92	40.63	2.27	0.55
137170	1999 HF1	0.82	0.46	8.03	44	(4)	4.1	16.6	1.01	43.20	1.30	0.80
163243	2002 FB3	0.76	0.60	11.88	33	(9)	4.1	18.1	0.93	45.71	0.57	2.86
2100	Ra-Shalom	0.83	0.44	7.50	52	(11)	4.2	17.7	0.71	47.87	1.62	4.38
87684	2000 SY2	0.86	0.64	9.57	81	(4)	4.4	18.4	0.67	49.75	2.55	0.54
	2005 GO21	0.75	0.34	8.81	53	(4)	4.0	18.3	0.65	51.39	0.94	1.68
433	Eros	1.46	0.22	1.57	94	(0)	3.5	14.0	0.54	52.85	5.52	0.03
66146	1998 TU3	0.79	0.48	9.11	59	(6)	4.4	16.6	0.49	53.69	1.29	0.84
163693	2003 CP20	0.74	0.32	9.05	40	(0)	4.0	18.1	0.42	54.70	2.08	1.06
137925	2000 BJ19	1.29	0.76	4.86	35	(10)	4.2	18.2	0.41	55.98	2.19	0.67
141484	2002 DB4	0.86	0.37	6.52	40	(8)	4.2	18.3	0.38	57.10	1.30	1.44
4953	1990 MU	1.62	0.66	2.02	151	(34)	4.6	17.7	0.35	58.08	6.54	0.15
12711	Tukmit	1.19	0.27	2.70	77	(10)	4.9	18.3	0.33	59.47	2.22	0.87
3753	Cruithne	1.00	0.52	5.25	79	(15)	4.4	18.3	0.30	60.40	0.62	1.09
5381	Sekhmet	0.95	0.30	4.81	155	(33)	4.8	18.5	0.28	61.48	0.86	3.13
99907	1989 VA	0.73	0.59	13.10	19	(6)	3.2	18.6	0.25	63.19	13.51	0.32
	2005 MB	0.98	0.79	10.71	40	(0)	4.3	19.5	0.25	64.03	7.05	0.31

n° IAU	Asteroid i name	a [au]	e	Perihelion shift $\dot{\omega}_{J_2^\circ}$ ["/100yr]	Gaia observations			Uncertainty increasing		Yarkovsky effect		
					number	arc [yr]	Mean V	factor in the fit of J_2° [%]	factor in the fit of J_2° [%]	σ_a^{Gaia} [$\times 10^{-4}$ auMyr]	$\ \dot{a}\ /\sigma_a^{Gaia}$ [$\times 10^{-4}$ auMyr]	
137924	2000 BD19	0.88	0.90	5.1×10^{-2}	34	(5)	4.4	19.0	61.42	61.42	6.25	0.35
66391	1999 KW4	0.64	0.69	1.5×10^{-2}	37	(10)	4.2	17.7	7.98	95.12	1.01	1.85
3200	Phaethon	1.27	0.89	1.4×10^{-2}	74	(15)	4.1	18.2	3.64	140.66	1.73	0.39
85953	1999 FK21	0.74	0.70	1.8×10^{-2}	44	(6)	4.9	19.5	1.09	165.85	1.27	11.15
137170	1999 HF1	0.82	0.46	4.2×10^{-3}	44	(4)	4.1	16.6	0.44	174.19	1.30	0.80
	2007 EP88	0.84	0.89	5.7×10^{-2}	37	(4)	4.0	19.9	0.42	185.34	97.89	0.04
2100	Ra-Shalom	0.83	0.44	4.4×10^{-3}	52	(11)	4.2	17.7	0.42	196.79	1.62	4.38
138127	2000 EE14	0.66	0.53	1.1×10^{-2}	28	(10)	4.1	18.5	0.37	213.20	1.86	1.13
99907	1989 VA	0.73	0.59	8.7×10^{-3}	19	(6)	3.2	18.6	0.37	225.15	13.51	0.32
1566	Icarus	1.08	0.83	1.1×10^{-2}	31	(7)	4.2	18.9	0.36	251.58	8.73	0.34
163243	2002 FB3	0.76	0.60	9.1×10^{-3}	33	(9)	4.1	18.1	0.35	264.97	0.57	2.86
87684	2000 SY2	0.86	0.64	7.2×10^{-3}	81	(4)	4.4	18.4	0.29	283.01	2.55	0.54
105140	2000 NL10	0.91	0.82	1.3×10^{-2}	72	(4)	4.2	18.8	0.24	321.26	2.27	0.55
	2005 GO21	0.75	0.34	4.5×10^{-3}	53	(4)	4.0	18.3	0.14	332.44	0.94	1.68
40267	1999 GJ4	1.34	0.81	3.0×10^{-3}	39	(0)	4.9	19.0	0.14	343.17	5.59	0.28
	2005 MB	0.98	0.79	5.8×10^{-3}	40	(0)	4.3	19.5	0.13	364.58	7.05	0.31
87309	2000 QP	0.85	0.46	2.9×10^{-3}	31	(8)	4.4	19.1	0.13	374.32	5.92	0.52
12711	Tukmit	1.19	0.27	6.0×10^{-4}	77	(10)	4.9	18.3	0.13	378.17	2.22	0.87
137925	2000 BJ19	1.29	0.76	2.6×10^{-3}	35	(10)	4.2	18.2	0.12	390.07	2.19	0.67
5381	Sekhmet	0.95	0.30	7.0×10^{-4}	155	(33)	4.8	18.5	0.09	395.79	0.86	3.13

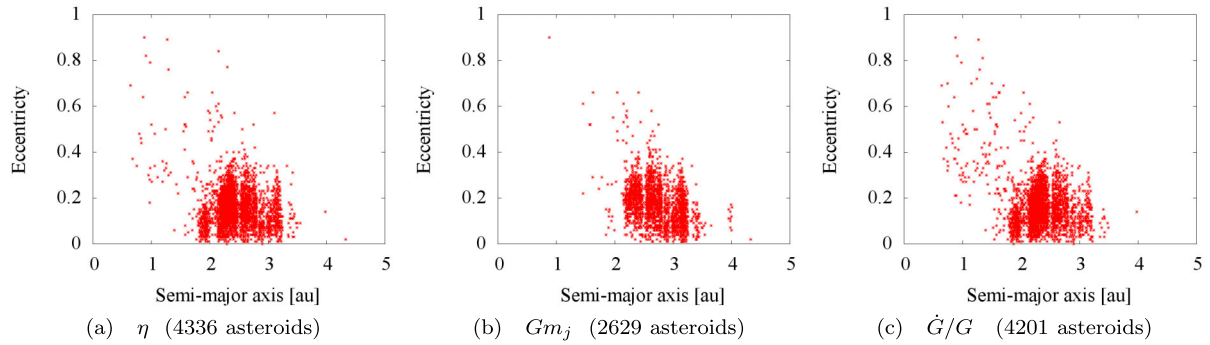


FIG. 3 (color online). Plots of orbital elements in semimajor axis vs. eccentricity space of the asteroids which, if they are not considered in the fit of the Nordtvedt parameter η (a), Gm of Jupiter (b) and \dot{G}/G (c), double the final derivation uncertainties listed in Table III—about half of the total information is contained in the Gaia observations of them.

$\sigma_{\eta}^M = 2.54 \times 10^{-3}$ only by considering this population, which is very close to the general result in Table III ($\sigma_{\eta} = 2.36 \times 10^{-3}$). On the other hand, the Trojan asteroids, well-known as privileged candidates to test a violation of the SEP (see Sec. IV D 1) are trifling for Gaia (too short observational time): the awaited observations of 1362 Trojans by the satellite will enable us only to achieve a precision of $\sigma_{\eta}^T = 1.25 \times 10^{-1}$, 2 orders of magnitude worse than the final uncertainty from all minor planets.

C. Planetary masses as unknown parameters

For the sake of curiosity, a variance analysis was applied to estimating the Gm of the eight planets and Pluto simultaneously. The expected formal precisions and comparison to other derivations are compiled in Table VII. None of planetary Gm_s are really worth measuring from the Gaia observation of minor planets except for Jupiter. Its estimate mostly depends on the main-belt asteroids that Gaia will observe (see Fig. 3(b)), which is an important point because, their dynamics being well-known, systematic errors will not be a problem in yielding an accurate measurement.

VI. CONCLUSION

As a conclusion, the results obtained were summarized and supplemented by the future work to be led for their improvement.

- (1) The future observations by the satellite Gaia will first enable us to extend the possibility to carry out accurate tests of fundamental physics by analyzing the astrometric observations of minor planets. The most relevant assessments concern the PPN parameter β , the temporal variation in the gravitational constant \dot{G}/G and the Nordtvedt parameter η . The addition of the Jovian Gm among the unknown parameters is of interest since it could be computed with a competitive formal precision. Furthermore, the results should be better, knowing that the Gaia astrometric precision used in the simulations is underestimated, and asteroid discoveries by the satellite could bring new significant constraints on certain parameters (e.g., well-observed new NEAs in the derivation of β). Two mission scenarios were also envisaged: a one-year delay should not

TABLE VII. Deriving the Gm of the eight planets and Pluto with Gaia.

Body j	Gm_j [au^3d^{-2}]	Gaia precision [au^3d^{-2}]	Current precision [au^3d^{-2}]	Estimation method references
Mercury	4.91×10^{-11}	1.43×10^{-15}	8.92×10^{-17}	Space probe [80]
Venus	7.24×10^{-10}	6.60×10^{-16}	1.34×10^{-17}	Space probe [81]
Earth	8.89×10^{-10}	3.46×10^{-16}	3.12×10^{-18}	Moon (LLR) ^a
Mars	9.55×10^{-11}	3.11×10^{-16}	6.24×10^{-19}	Space probes [82]
Jupiter	2.82×10^{-07}	2.83×10^{-15}	3.35×10^{-15}	Natural satellites ^b
Saturn	8.46×10^{-08}	3.26×10^{-14}	2.45×10^{-15}	Natural Satellites and Space probes [83]
Uranus	1.29×10^{-08}	3.37×10^{-13}	1.34×10^{-14}	Natural satellites [84]
Neptune	1.52×10^{-08}	1.20×10^{-12}	2.23×10^{-14}	Space probe and Natural satellites [85]
Pluto	1.95×10^{-12}	1.57×10^{-12}	8.25×10^{-15}	Natural satellites [86]

^aFolkner, W. M. and Williams, J. G. 2008. "GM parameters and uncertainties in planetary ephemeris DE421." Interoffice Memo. 343R-08-004 (internal document), Jet Propulsion Laboratory, Pasadena, CA.

^bJacobson, R. A. 2005. "Jovian Satellite ephemeris-JUP230" private communication.

significantly change the results, while a one-year extension would allow us to reduce the derivation uncertainties by factors within 1.9–3.7. In addition, several parameters have already accurately measured by other methods, and then a discrepancy from the Gaia derivation may be a valuable alert about the correctness of the dynamical model used.

- (2) The asteroids on which the parameter estimations with Gaia rest were listed. Thus, we can better know where our efforts have to be directed in order to improve the measurement accuracy. Near-Earth asteroids, which are essential for some tests of general relativity, are the main motivation for such a list. They are well-known to be very sensitive to the nongravitational Yarkovsky effect, the modelling of which is tricky because the knowledge of many physical parameters hard to estimate, is required. Having identified the most promising candidates for tests of GR, we can define the parameters to be derived, the observation campaigns to be consequently led, and the accurate radar observations from the ground that we can combine with the Gaia data to improve the derivation precision. The impact of the Gaia stellar catalogue is another point to take into consideration. It will allow us to improve the reduction procedure of ground-based observations, and so, the accuracy of reduced data; in consequence, introducing new reduced observations showing a good precision could be an interesting subject to be investigated.
- (3) The inquiry into the test of the Nordtvedt effect is far from finished: the impact of the nonstationarity of the Sun will be studied given that the Sun experiences radial oscillations.

ACKNOWLEDGMENTS

S. Mouret thanks M. Soffel for his valuable remarks, W.M. Folkner for the information about planetary ephemerides and the referees for their relevant comments. S. Mouret acknowledges the support of the Deutsche Forschungsgemeinschaft (German Research Foundation).

APPENDIX A: SECULAR EFFECT FROM THE TEMPORAL VARIATION OF G

The largest secular effect from a linear temporal variation of G is in the mean anomaly M because the attraction of the Sun dominates in the solar system. In the classical two-body problem, the linear variation in time of G can be considered as a perturbation deriving from the potential

$$U_{\dot{G}} = \frac{\dot{G}(t - t_0)}{r} m_{\odot}. \quad (\text{A1})$$

In order to estimate the first-order secular terms in the perturbations of the osculating elements, we average the potential $U_{\dot{G}}$ over the fast changing angular variables to remove the periodic effects due to $1/r$. The averaged potential has the form

$$\begin{aligned} [U_{\dot{G}}] &= \frac{1}{2\pi} \int_0^{2\pi} \frac{\dot{G}(t - t_0)}{r} m_{\odot} dM, \\ &= \frac{1}{2\pi} \int_0^{2\pi} \frac{\dot{G}(t - t_0)}{a} m_{\odot} dE, \end{aligned}$$

where E is the eccentric anomaly. The integration is direct when considering $\dot{G}(t - t_0)$ as a constant: \dot{G}/G is precisely estimated to $(4 \pm 9) \times 10^{-13}$ a year [47], which is very small in comparison with the variation of the heliocentric distance r of the body. The effective general averaging principle with slowly varying parameters [87] gives

$$[U_{\dot{G}}] \sim \frac{\dot{G}(t - t_0)}{a} m_{\odot}. \quad (\text{A2})$$

In the Lagrange's planetary equations, the averaged potential in Eq. (A2) implies that only the mean anomaly is secularly perturbed, at the rate of

$$\frac{dM}{dt} = -\frac{2}{na} \frac{\partial [U_{\dot{G}}]}{\partial a}, \quad (\text{A3})$$

where n is the mean motion of the celestial body at the time t_0 . At the time t , the mean anomaly M will have thus changed by

$$\Delta M = \int_{t_0}^t -\frac{2}{na} \frac{\partial [U_{\dot{G}}]}{\partial a} dt = n \frac{\dot{G}}{G} m_{\odot} (t - t_0)^2. \quad (\text{A4})$$

-
- [1] F. Mignard, A. Cellino, K. Muinonen, P. Tanga, M. Delbò, A. Dell'Oro, M. Granvik, D. Hestroffer, S. Mouret, W. Thuillot *et al.*, *Earth Moon Planets* **101**, 97 (2008).
 [2] J. J. Gilvarry, *Publ. Astron. Soc. Pac.* **65**, 173 (1953).
 [3] J. J. Gilvarry, *Phys. Rev.* **89**, 1046 (1953).
 [4] J. H. Lieske and G. W. Null, *Astron. J.* **74**, 297 (1969).
 [5] I. I. Shapiro, M. E. Ash, and W. B. Smith, *Phys. Rev. Lett.* **20**, 1517 (1968).
 [6] I. I. Shapiro, W. B. Smith, M. E. Ash, and S. Herrick, *Astron. J.* **76**, 588 (1971).
 [7] G. Sitarski, *Astron. J.* **104**, 1226 (1992).
 [8] R. H. Dicke, *Astrophys. J.* **70**, 395 (1965).
 [9] K. Nordtvedt, *Phys. Rev.* **169**, 1014 (1968).

- [10] R. B. Orellana and H. Vucetich, *Astron. Astrophys.* **200**, 248 (1988).
- [11] R. B. Orellana and H. Vucetich, *Astron. Astrophys.* **273**, 313 (1993).
- [12] URL:<ftp://ftp.lowell.edu/pub/elgb/astorb.html>.
- [13] S. Mouret and F. Mignard, *Mon. Not. R. Astron. Soc.* **413**, 741 (2011).
- [14] U. J. Leverrier, *Annals de l'Observatoire de Paris* **5**, 1 (1859).
- [15] P. Harzer, *Astron. Nachr.* **127**, 81 (1891).
- [16] S. Newcomb, *The Elements of The Four Inner Planets* (Government Printing Office, Washington, 1895).
- [17] R. H. Dicke and H. M. Goldenberg, *Astrophys. J. Suppl. Ser.* **27**, 131 (1974).
- [18] W. Landgraf, *Sol. Phys.* **142**, 403 (1992).
- [19] S. Pireaux and J.-P. Rozelot, *Astrophys. Space Sci.* **284**, 1159 (2003).
- [20] E. Bois and J. F. Girard, *Celest. Mech. Dyn. Astron.* **73**, 329 (1999).
- [21] E. V. Pitjeva, *Solar System Research* **39**, 176 (2005).
- [22] A. Fienga, J. Laskar, T. Morley, H. Manche, P. Kuchynka, C. Le Poncin-Lafitte, F. Budnik, M. Gastineau, and L. Somenzi, *Astron. Astrophys.* **507**, 1675 (2009).
- [23] J.-P. Rozelot and S. Lefebvre, in *The Sun's Surface and Subsurface: Investigating Shape*, edited by J.-P. Rozelot, Lecture Notes in Physics (Berlin Springer Verlag, vol. 599, 2003), pp. 4–27.
- [24] J. P. Rozelot, C. Damiani, and S. Lefebvre, *J. Atmos. Sol. Terr. Phys.* **71**, 1683 (2009).
- [25] J. Benkhoff, J. van Casteren, H. Hayakawa, M. Fujimoto, H. Laakso, M. Novara, P. Ferri, H. R. Middleton, and R. Ziethe, *Planet. Space Sci.* **58**, 2 (2010).
- [26] W. Ni, *Int. J. Mod. Phys. D* **17**, 921 (2008).
- [27] M. E. Davies, V. K. Abalakin, M. Bursa, J. H. Lieske, B. Morando, D. Morrison, P. K. Seidelmann, A. T. Sinclair, B. Yallop, and Y. S. Tjuflin, *Celest. Mech. Dyn. Astron.* **63**, 127 (1995).
- [28] D. D. McCarthy, IERS Technical Report No. 13/JUL, 1992, 1992.
- [29] C. M. Will and K. J. Nordtvedt, *Astrophys. J.* **177**, 757 (1972).
- [30] G. A. Seielstad, R. A. Sramek, and K. W. Weiler, *Phys. Rev. Lett.* **24**, 1373 (1970).
- [31] D. O. Muhleman, R. D. Ekers, and E. B. Fomalont, *Phys. Rev. Lett.* **24**, 1377 (1970).
- [32] S. S. Shapiro, J. L. Davis, D. E. Lebach, and J. S. Gregory, *Phys. Rev. Lett.* **92**, 121101 (2004).
- [33] S. B. Lambert and C. Le Poncin-Lafitte, *Astron. Astrophys.* **529**, A70 (2011).
- [34] I. I. Shapiro, *Phys. Rev. Lett.* **13**, 789 (1964).
- [35] E. Fomalont, S. Kopeikin, G. Lanyi, and J. Benson, *Astrophys. J.* **699**, 1395 (2009).
- [36] B. Bertotti, L. Iess, and P. Tortora, *Nature (London)* **425**, 374 (2003).
- [37] B. Bertotti, N. Ashby, and L. Iess, *Classical Quantum Gravity* **25**, 045013 (2008).
- [38] S. M. Kopeikin, *Phys. Lett. A* **373**, 2605 (2009).
- [39] E. V. Pitjeva, *Astron. Lett.* **31**, 340 (2005).
- [40] E. V. Pitjeva, in *IAU Colloq. 196: Transits of Venus: New Views of the Solar System and Galaxy*, edited by D. W. Kurtz (Astronomical Society of the Pacific, Orem, UT, 2005), pp. 230–241.
- [41] A. Milani, D. Vokrouhlický, D. Villani, C. Bonanno, and A. Rossi, *Phys. Rev. D* **66**, 082001 (2002).
- [42] S. G. Turyshev, M. Shao, K. L. Nordtvedt, H. Dittus, C. Laemmerzahl, S. Theil, C. Salomon, S. Reynaud, T. Damour, U. Johann *et al.*, *Exp. Astron.* **27**, 27 (2009).
- [43] D. Hobbs, B. Holl, L. Lindegren, F. Raison, S. Klioner, and A. Butkevich, in *IAU Symposium*, edited by S. A. Klioner, P. K. Seidelmann, and M. H. Soffel (2010), vol. 261 of IAU Symposium, pp. 315–319.
- [44] M. Froeschle, F. Mignard, and F. Arenou, in *Hipparcos–Venice '97* (1997), vol. 402 of ESA Special Publication.
- [45] A. Fienga, H. Manche, J. Laskar, and M. Gastineau, *Astron. Astrophys.* **477**, 315 (2008).
- [46] C. Will, *Theory and experiment in gravitational physics* (Cambridge University Press, Cambridge, England, 1993), 2nd ed..
- [47] J. G. Williams, S. G. Turyshev, and D. H. Boggs, *Phys. Rev. Lett.* **93**, 261101 (2004).
- [48] V. A. Brumberg, *Relativistic celestial mechanics*. (1972).
- [49] S. Weinberg, *Gravitation and Cosmology: Principles and Applications of the General Theory of Relativity* (Wiley, New York, 1972).
- [50] R. H. Dicke and C. Brans, *Phys. Rev.* **124**, 925 (1961).
- [51] J. G. Williams and W. M. Folkner, American Astronomical Society, IAU Symposium #261. Relativity in Fundamental Astronomy: Dynamics, Reference Frames, and Data Analysis (Virginia Beach, Virginia 2009); *Bull. Am. Astron. Soc.* **41**, 882 (2009).
- [52] J. G. Williams, S. G. Turyshev, and T. W. Murphy, *Int. J. Mod. Phys. D* **13**, 567 (2004).
- [53] C. M. Will, *Living Rev. Relativity* **9**, 3 (2006).
- [54] R. W. Hellings, P. J. Adams, J. D. Anderson, M. S. Keesey, E. L. Lau, E. M. Standish, V. M. Canuto, and I. Goldman, *Phys. Rev. Lett.* **51**, 1609 (1983).
- [55] S. Mouret, D. Hestroffer, and F. Mignard, *Astron. Astrophys.* **472**, 1017 (2007).
- [56] S. Mouret, J. L. Simon, F. Mignard, and D. Hestroffer, *Astron. Astrophys.* **508**, 479 (2009).
- [57] J. Mestschersky, *Astron. Nachr.* **132**, 129 (1893).
- [58] J. Mestschersky, *Astron. Nachr.* **159**, 229 (1902).
- [59] J. P. Vinti, *Mon. Not. R. Astron. Soc.* **169**, 417 (1974).
- [60] R. V. Eötvös, D. Pekár, and E. Fekete, *Ann. Phys. (Leipzig)* **373**, 11 (1922).
- [61] P. G. Roll, R. Krotkov, and R. H. Dicke, *Ann. Phys. (N.Y.)* **26**, 442 (1964).
- [62] E. G. Adelberger, *Classical Quantum Gravity* **18**, 2397 (2001).
- [63] S. Schlamminger, K.-Y. Choi, T. A. Wagner, J. H. Gundlach, and E. G. Adelberger, *Phys. Rev. Lett.* **100**, 041101 (2008).
- [64] J. D. Anderson, M. Gross, K. L. Nordtvedt, and S. G. Turyshev, *Astrophys. J.* **459**, 365 (1996).
- [65] C. W. Allen, *Astrophysical Quantities* (London: Athlone, 1985), edited by, 3.
- [66] B. Carry, C. Dumas, M. Fulchignoni, W. J. Merline, J. Berthier, D. Hestroffer, T. Fusco, and P. Tamblyn, *Astron. Astrophys.* **478**, 235 (2008).
- [67] R. H. Dicke, in *Gravitation and Relativity*, edited by, H.-Y. Chiu and W. F. Hoffman (1964).
- [68] K. Nordtvedt, *Phys. Rev.* **169**, 1017 (1968).
- [69] K. Nordtvedt, Jr., *Rep. Prog. Phys.* **45**, 631 (1982).
- [70] R. K. Ulrich, *Astrophys. J.* **258**, 404 (1982).

- [71] K. Nordtvedt, *Phys. Rev.* **170**, 1186 (1968).
- [72] J.G. Williams, S.G. Turyshev, and D.H. Boggs, *Int. J. Mod. Phys. D* **18**, 1129 (2009).
- [73] T.W. Murphy, E.G. Adelberger, J.B.R. Battat, L.N. Carey, C.D. Hoyle, P. Leblanc, E.L. Michelsen, K. Nordtvedt, A.E. Orin, J.D. Strasburg *et al.*, *Publ. Astron. Soc. Pac.* **120**, 20 (2008).
- [74] A.R. Plastino and H. Vucetich, *Astron. Astrophys.* **262**, 321 (1992).
- [75] E. Bowell, B. Hapke, D. Domingue, K. Lumme, J. Peltoniemi, and A.W. Harris, in *Asteroids II*, edited by R.P. Binzel, T. Gehrels, and M.S. Matthews (1989), pp. 524–556.
- [76] S. Kopeikin and I. Vlasov, *Phys. Rep.* **400**, 209 (2004).
- [77] D. Vokrouhlický, *Astron. Astrophys.* **335**, 1093 (1998).
- [78] D. Vokrouhlický, *Astron. Astrophys.* **344**, 362 (1999).
- [79] S.R. Chesley and D. Vokrouhlicky, in *AAS/Division of Dynamical Astronomy Meeting* (American Astronomical Society, Washington, DC 2008), vol. 39, pp. 02.04.
- [80] D.E. Smith, M.T. Zuber, R.J. Phillips, S.C. Solomon, G.A. Neumann, F.G. Lemoine, S.J. Peale, J. Margot, M.H. Torrence, M.J. Talpe *et al.*, *Icarus* **209**, 88 (2010).
- [81] A.S. Konopliv, W.B. Banerdt, and W.L. Sjogren, *Icarus* **139**, 3 (1999).
- [82] A.S. Konopliv, C.F. Yoder, E.M. Standish, D. Yuan, and W.L. Sjogren, *Icarus* **182**, 23 (2006).
- [83] R.A. Jacobson, P.G. Antreasian, J.J. Bordi, K.E. Criddle, R. Ionasescu, J.B. Jones, R.A. Mackenzie, M.C. Meek, D. Parcher, F.J. Pelletier *et al.*, *Astron. J.* **132**, 2520 (2006).
- [84] R.A. Jacobson, in *Bulletin of the American Astronomical Society* (2007), vol. 38 of, pp. 453–+.
- [85] R.A. Jacobson, *Astron. J.* **137**, 4322 (2009).
- [86] D.J. Tholen, M.W. Buie, W.M. Grundy, and G.T. Elliott, *Astron. J.* **135**, 777 (2008).
- [87] V.I. Arnold, *Graduate texts in mathematics* (Springer, New York, 1978).